POWER CONTROL OF A FLASHLAMP-BASED HEATING SOLUTION FOR AUTOMATED DRY FIBRE PLACEMENT

Philippe Monnot[1], David Williams[2] & Mattia Di Francesco[1]
[1] National Composites Centre, Bristol & Bath Science Park, Emersons Green, Bristol BS16 7FS, UK
Web Page: www.nccuk.com
Email: Philippe.Monnot@nccuk.com & Mattia.DiFrancesco@nccuk.com
[2] Heraeus Noblelight Ltd., Cambridge Science Park, Milton Road, Cambridge, CB4 0GQ, UK
Web Page: www.heraeus.com
Email: David.Williams@heraeus.com
Keywords: Automated Fibre Placement, Flashlamp, Diode laser, Dry fibre, Power control

Abstract

The growing demand for modern commercial aircraft requires a step change in the manufacturing rate of composite components. Automated Fibre Placement is widely recognised as one of the automated processes with the potential to deliver such increase. Adopting a robust heating source is critical to unlock the potential of this technology. The novel *humm3*™ radiates the material with intermittent high-energy flashes, promising to deliver a more controllable and versatile process. Adopting a new heating technology requires the definition of a new power control function in order to maintain the specified nip-point temperature steady independently of the layup speed. This study applies a previously developed power control definition procedure to the *humm3*™/bindered dry fibre combination, compares it with an established heating system and proposes an effective process flow for the implementation of the procedure. The proposed method has the potential to decrease the development time for manufacturers wishing to explore the Automated Fibre Placement's potential.

1. Introduction

Automated Fibre Placement (AFP) is an automated additive manufacturing process. A purposely designed end-effector mounted on a robotic manipulator is used to layup the material, layer by layer, over a tool. The combined action of temperature and pressure ensures that the incoming material is adhered to the substrate [1]. The latest generation commercial aircraft integrate a variety of composites primary structures, some which are currently manufactured with this process, e.g. wing covers, fuselage barrels, wing spars, etc. The growing demand requires manufacturers to increase their production rates, therefore by stretching the capabilities of their automated manufacturing processes [1].

The novel *humm3*™ heating system has the potential to expand the capabilities of current and future AFP machines by providing a versatile and controllable heating system [2]. It uses high-energy pulsed flashes to heat the incoming material and substrate. The system is controlled through three independent parameters (pulse frequency, amplitude and duration), which can tailor the heat flux to the material and process specific requirements. A large range of materials can be deposited using the *humm3*™ [2]: thermoset prepregs (40 to 60 °C [3]), bindered dry fibres (160 to 200 °C [3]), and thermoplastic prepregs (275 to 350 °C [3]).

Implementing a new heating system requires the manufacturer to invest in the development of the process knowledge required to benefit from the new technology. Among others, the power control function must be redefined. This relates the heater's output power P to the AFP machine's layup speed V to maintain the process temperature constant during layup. Di Francesco *et al.* [4] proposed an

empirical procedure to determine the relationship between P and V. This requires surface temperature measurements of the substrate at the nip-point T_{vnp} at different V and for a range of P. A semi-empirical procedure was also suggested to reduce to a minimum the number of mandatory tests. However, these methods were only demonstrated for a diode laser, an industry well established heating system.

Therefore, the purpose of this study was to apply these procedures to the layup of bindered dry fibres using the *humm3*™ heating system (objective #1). The same methodology was also applied to the diode laser, which aimed to highlight similarities and/or differences between both heating systems (objective #2). Finally, a process flow that clearly indicates how to generate a power control function was defined (objective #3).

2. Theoretical background

Di Francesco *et al.*'s method is founded on Eq. (1), an analytical solution to a one-dimensional transient thermal problem that idealizes the substrate as a semi-infinite solid [4]. This analytical relationship relates the substrate's surface temperature T_s, V, P, the material thermal properties K_M, the heater's setup K_S as well as the initial temperature of the substrate T_0.

$$T_s(P,V) = K_M K_S V^{-0.5} P + T_0;\ K_m = 2a/\sqrt{\rho c_p k(T)\pi}\ ;\ K_S = h_1/\sqrt{h_1'}wh \tag{1}$$

K_M is a function of the material's thermal conductivity k, density ρ, heat capacity c_p and surface absorptance a. K_S is function of the percentage power delivered to the substrate h_1/h, the width of the substrate heated area w and the length of the substrate heated area h_1'. Figure 1 illustrates the setup for the *humm3*™ and the diode laser. Eq. (1) assumes zero heat losses, thus all the energy is used to heat up the material. From experimental observations, Di Francesco *et al.* proposed that T_{vnp} could be a linear function of P. Therefore,

$$T_{vnp}(P,V) = m(V)P + c(V) \tag{2}$$

where the slope m and the intercept c are both function of V. This assumption is valid in the material's temperature range of interest. The range limits are respectively the minimum temperature required for the substrate and the incoming tape to bond, and the highest temperature that does not cause apparent degradation of the material. As shown in Eq. (3), P can now be expressed as a function of any combination of T_{vnp} and V. $m(V)$ and $c(V)$ are determined empirically by measuring the nip-point temperature for a number of combinations of P and V.

$$P\big(V, T_{vnp}\big) = \frac{T_{vnp} - c(V)}{m(V)} \tag{3}$$

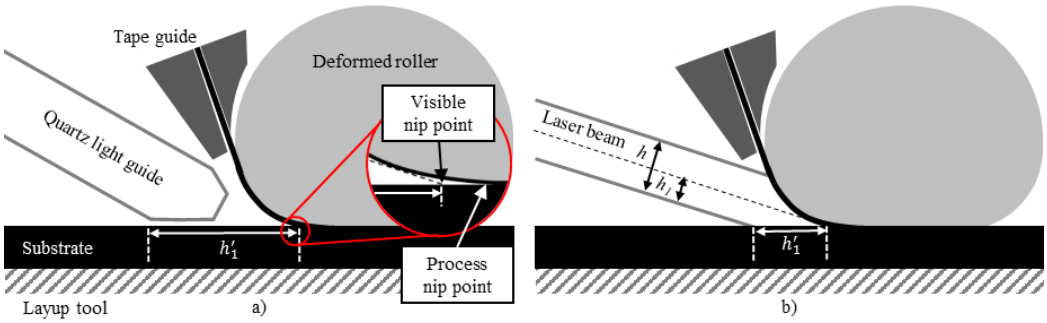

Figure 1. Automated Fibre Placement (AFP) deposition schematic for each heating system: a) *humm3*™; b) Diode laser [4].

3. Experimental setup

3.1. Machine and materials

A *Coriolis Composites SAS* AFP machine was used to process *Hexcel HiTape*® bindered dry fibre tapes (210 g/m^2). The material comes in the form of a 6.35 mm unidirectional tape made from carbon fibres (*Hexcel HexTow*® *IMA*) held together by a thermoplastic veil [5].

3.2. Heating systems

The *humm3*™, shown in Figure 2a was equipped with a 6 kW power (input) unit. The manufacturer estimated the system's input to output power ratio to ~50 %. The lamp contains xenon gas, which has a high electric resistance at ambient temperature. Under a high voltage, it ionizes, therefore allowing it to conduct electricity. The power generator capacitors are then discharged at regular intervals to generate the flashes: short-duration energy pulses with high average power and a broad spectral content ($\lambda \approx 200 - 1050\ nm$) [2]. The pulse duration, voltage and frequency are controlled independently. A quartz light guide installed in front of the lamp acts as an optical medium to focus the generated rays in vicinity of the nip-point. As shown in Figure 2a, the end of the quartz bloc was chamfered to distribute the energy to the incoming tape and substrate. The fibre-coupled diode laser from *Laserline GmbH (LDF 6000-100)*, shown in Figure 2b, has a 3 kW power (output) generator (2 diode stacks, $\lambda = 1025 \pm 10\ nm$) [6]. The homogeniser optic produces a 8 × 57 mm rectangular spot.

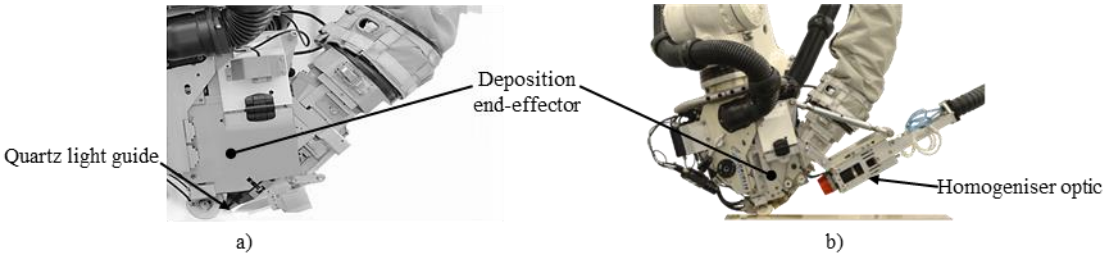

Figure 2. Heating systems installed on a *Coriolis Composites SAS* AFP machine: a) *humm3*™ [2]; b) *Laserline GmbH* 6 kW diode laser.

For each heating system, K_S was calculated and reported in Table 1. h_1/h is determine geometrically for the diode laser and from ray tracing analysis for the *humm3*™.

Table 1. Setup dependant coefficient K_S for each heating system

Heating system	h_1/h (%)	*w (mm)*	h_1' *(mm)*	K_S $(m^{-0.5})$
humm3™	60	55	53.0	47.4
Diode laser (6 kW) - 8 X 57 mm	70	57	18.1	91.2

3.3. Temperature measurements

The surface temperature of the substrate was measured using a FLIR A325 (λ = 7.5 – 13 μm) thermal camera with a resolution of 320 × 240 pixels at 60 Hz. For each image, T_{vnp} was measured along a line composed of 200 individual points positioned along the visible nip-point. The apparent emissivity of the material in the temperature range of interest (150 – 300 °C, experimentally determined) was computed according to the ASTM E1933 standard [7]. Tests were conducted using a purposely designed test rig, which reproduces the lay-up geometry, the thermal camera position and orientation, and the environmental conditions. The apparent emissivity was found to be 0.85 across the temperature range of interest.

4. Power control procedures

4.1. Empirical procedure

The empirical procedure steps developed by Di Francesco *et al.* [4] and followed in this study are:

- Step 1: Measure T_{vnp} for a range of P (two to five in this case) at a range of V (five in this case) that covers the operation spectrum (64 to 1000 mm/s in this case);
- Step 2: For each V, determine the slope $m_{T_{vnp}-P}$ and the intercept $c_{T_{vnp}-P}$ of the T_{vnp} against P linear regression;
- Step 3: Eq. (3) intercept $c(V)$ is approximated by conducting a linear regression analysis of $c_{T_{vnp}-P}$ against V:

$$c(V) = m_{c_{T_{vnp}-P}-V} V + c_{c_{T_{vnp}-P}-V} \tag{4}$$

- Step 4: Eq. (3) slope $m(V)$ is approximated by conducting a power regression analysis of $m_{T_{vnp}-P}$ against V:

$$m(V) = A_{m_{T_{vnp}-P}-V} V^{B_{m_{T_{vnp}-P}-V}} \tag{5}$$

- Step 5: Eq. (4) and (5) are substituted in Eq. (3), which establishes the empirical power control function:

$$P(V, T_{vnp}) = \frac{T_{vnp} - (m_{c_{T_{vnp}-P}-V} V + c_{c_{T_{vnp}-P}-V})}{A_{m_{T_{vnp}-P}-V}} V^{-B_{m_{T_{vnp}-P}-V}} \tag{6}$$

For each power and layup speed combination (P,V), T_{vnp} was measured for at least 25 points along the layup of an eight tapes wide course over a substrate no thinner than five plies. The deposition compaction force was set up to 200 N (nominal) for all the tests. For the *humm3*™ trials conducted as part of this study, only the pulse duration was varied to modulate the output power. The pulse frequency was set to 60 Hz and voltage to 200 V. The empirical power control function was computed with a target T_{vnp} set to 225 ℃ (T_{target}). The V range was set between 64 mm/s and 1000 mm/s, which covers the typical operation spectrum.

Figure 3 and Figure 4 present results from step one to four of the empirical procedure for each heating system. As opposed to the diode laser (Figure 4b), the *humm3*™ regression slopes $m_{T_{vnp}-P}$ do not exhibit a strong power behaviour, thus not significantly changing with V (Figure 3b). Therefore, the P increment required to increase T_{vnp} by a certain amount appears to be constant with V. Comparing Figure 3a and Figure 4a, the *humm3*™ requires significantly more power than the diode laser to reach the same T_{target}. As presented in Table 1, the *humm3*™ has a larger heating area than the diode laser, which necessitates more P to obtain the same surface heat flux. A larger heating area also means that the *humm3*™ heats up the material further away from the nip-point, thus for a longer time. This difference makes the *humm3*™ less affected by low material exposure time at higher V. Combined with material variability and uneven substrate thickness, the larger hearting area causes more variability of the measured T_{vnp} across the nip-point area and along a course. Consequently, the *humm3*™ T_{vnp} against P linear regression confidence intervals are larger than the diode laser ones and average r-squared value lower (Figure 3a and Figure 4a). Figure 5 presents the resulting empirical power control function for each heating system. The coefficients are listed in Table 2. As expected, the *humm3*™ requires significantly more power than the diode laser to reach 225 ℃.

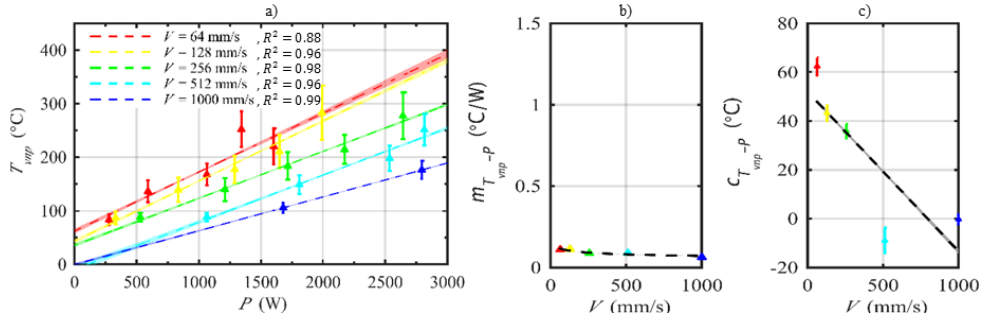

Figure 3. *humm3*™ a) Measured nip-point temperature T_{vnp} for a range of output powers P; b) Linear regression slopes $m_{T_{vnp}-P}$ as function of layup speed V; c) Linear regression intercepts $c_{T_{vnp}-P}$ as function of layup speed V. (Error bars and shaded areas indicate 95 % confidence intervals [8])

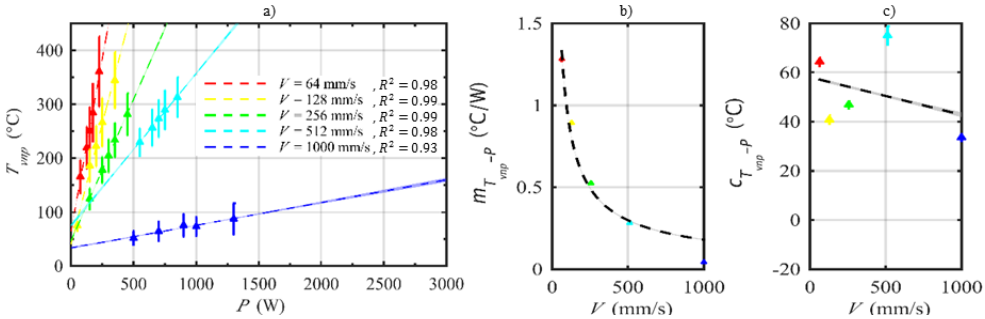

Figure 4. Diode laser (8 × 57 mm): a) Measured nip-point temperature T_{vnp} for a range of output powers P; b) Linear regression slopes $m_{T_{vnp}-P}$ as function of layup speed V; c) Linear regression intercepts $c_{T_{vnp}-P}$ as function of layup speed V. (Error bars and shaded areas indicate 95 % confidence intervals [8])

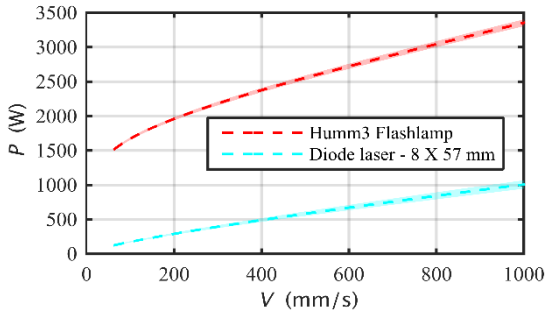

Figure 5. Empirical power control function for the *humm3*™ and the diode laser (8 × 57 mm) for a target nip-point temperature T_{target} of 225 °C. (Shaded area represents the 95 % confidence interval [8])

Table 2. Empirical power control function coefficients for the *humm3*™ and diode laser for a target nip-point temperature T_{target} of 225 °C.

		humm3™		*Diode laser*	
Coefficients	*Units*	*Mean*	*SD*	*Mean*	*SD*
$A_{m_{T_{vnp}-P-V}}$	$°C/W$	2.45E-01	1.54E-03	2.71E01	3.12E-01
$B_{m_{T_{vnp}-P-V}}$	$\ln(°C/W)/\ln(mms^{-1})$	-1.79E-01	1.18E-03	-7.25E-01	2.51E-03
$m_{c_{T_{vnp}-P-V}}$	$°C/mms^{-1}$	-6.55E-02	6.33E-04	-1.53E-02	5.99E-04
$c_{c_{T_{vnp}-P-V}}$	°C	5.21E01	3.29E-01	5.81E01	3.11E-01

4.2. Alternative procedures

4.2.1. Analytical and analytical-corrected

Eq. (3) defines the analytical power control function. T_{target} was set to 225 °C and T_0 equal to 20 °C. K_M was extrapolated using Section 3.1 linear regression for T equal to T_{vnp}. K_m for *HiTape*® was computed at seven discrete temperatures, between 0 and 300 °C. It uses material thermal properties sourced from literature [9–11] and assumes the preform fibre volume fraction to be 44.5 % [3]. K_m can be approximated to vary as a linear function of the temperature in the 0 – 300 °C range (K_M = -1.9E-06T + 1.7E-03, R^2 = 0.99). K_S for each heating system can be found in Table 1.

According to Eq. (2), T_{vnp} against P for a given V is linear. However, it does not take into account the effect of temperature on the material's thermal properties. The analytical-corrected procedure considers this effect. Thus, T_{vnp} against P can be approximated as linear in the material's temperature range of interest (150 – 300 °C, Figure 6 red boxes). The linear regressions' intercepts all converge at one point, which corresponds to the apparent substrate temperature, $T_{0,app}$. As shown in Figure 6, $T_{0,app}$ is the same for *humm3*™ and the diode laser. This suggests that $T_{0,app}$ is a heating system independent parameter. An apparent K_M, $K_{M,app}$, also can be determined from Figure 6 linear regressions' slopes. For the analytical-corrected procedure, T_0 and K_M from Eq. (1) were respectively set to $T_{0,app}$ and $K_{M,app}$.

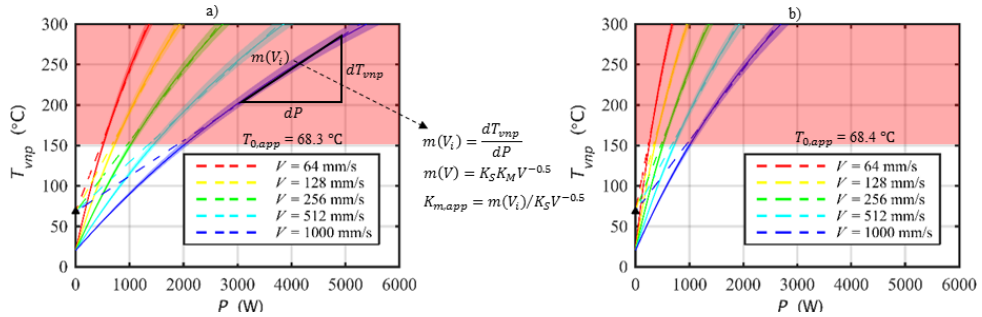

Figure 6. Analytical nip-point temperature T_{vnp} against P for tested layup speeds V (shaded area represents the 95% confidence interval [8]). Linear regression over the material's temperature range of interest to determine the apparent substrate temperature $T_{0,app}$: a) *humm3*™; b) Diode laser (8 × 57 mm).

4.2.2.Semi-empirical procedure

The semi-empirical procedure follows the empirical procedure's steps. However, step 2 linear regressions' intercepts $c_{T_{vnp}-P}$ are set equal to $T_{0,app}$. Therefore, step 1 only requires one P per V. Since $T_{0,app}$ is valid over the temperature range of interest, each (P, V) combination must be carefully selected. By setting Eq. (4) T_{vnp} to the temperature range of interest range limits, a P range is determined. For each V, P should be taken in the middle of the P range. At least three (P, V) combinations are necessary to cover the complete operation spectrum: minimum, middle and maximum V values. The semi-empirical power control function is computed by following the remaining empirical procedure steps. An extra set of experiments using the *humm3*™ were performed to validate this procedure. Tests were ran at different (P, V) combinations from the ones used to determine the empirical power control function: (48 mm/s, 995 W), (192 mm/s, 1897 W) and (400 mm/s, 2768 W).

4.3. Procedures comparison

Figure 7 presents the expected nominal nip-point temperature error $T_{vnp}\ error$ as function of V for each alternative procedure and heating system. In other words, if the alternative power control functions were

to be used, how far from T_{target} would the T_{vnp} across the V range. Figure 7b shows that both analytical power control functions for the diode laser are not good approximations of the empirical power control function. Thus, they overshot by more than 100 % under 400 mm/s. Di Francesco *et al.* [4] observed the same phenomenon and suggested that the constant material properties through the thickness of the substrate assumption doesn't hold true. However, the *humm3*™ analytical power control functions presented in Figure 7a provides a better approximation. This could be explained by the material's longer exposure time to the heat flux, since the *humm3*™ heats up the material further away from the nip-point. Therefore, the substrate's bulk temperature can be expected to be more uniform through its thickness when it gets to the nip-point. Hence, meeting the analytical model's assumption. However, this model must be used with great care. Its accuracy is highly depend on how the heated area is defined, K_s, especially for the *humm3*™. Due to the multiple emitting surfaces and their different distances to the material, it is most likely that the uniform heat flux and no energy losses assumptions don't hold true. This phenomenon should be properly investigated to increase the analytical procedure's accuracy.

Figure 7a shows that the *humm3*™ semi-empirical power control function doesn't provide a good approximation to the empirical power control function by overshooting T_{target} by ~20 %. Furthermore, Figure 7c shows that the T_{vnp} $error$ range increases with T_{target}. From Figure 3a, setting $T_{0,app}$ as $c_{T_{vnp}-P}$ for all V is not in agreement with experimental results: *humm3*™ regression slopes $m_{T_{vnp}-P}$ are mostly parallel and intercepts $c_{T_{vnp}-P}$ decrease linearly with V. Although Di Francesco et al. [4] presented good results for the diode laser, the semi-empirical procedure's assumption doesn't seem to be valid for the *humm3*™. A combination of the analytical (select the (P, V) combinations) and empirical procedures should therefore be the preferred approach for the *humm3*™.

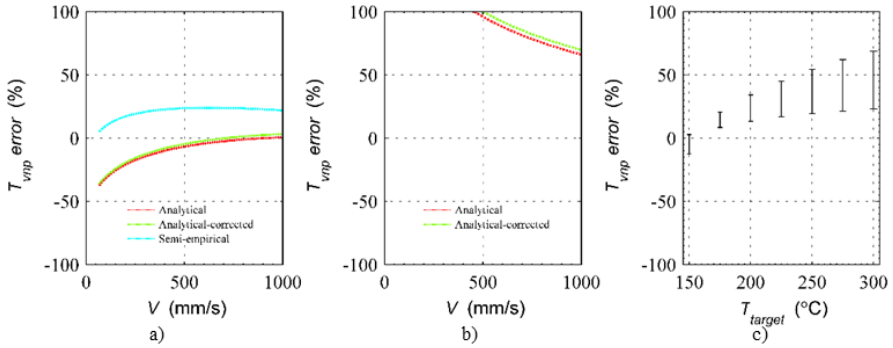

Figure 7. Expected nominal nip-point temperature T_{vnp} error (%) as function of lay-up speed V for each computed power control procedure: a) *humm3*™; b) Diode laser (8 × 57 mm) c) Semi-empirical power control function T_{vnp} $error$ range as function of T_{target}.

5. Power control function generation process flow

Figure 8 maps, from left to right, the different power control function generation processes.

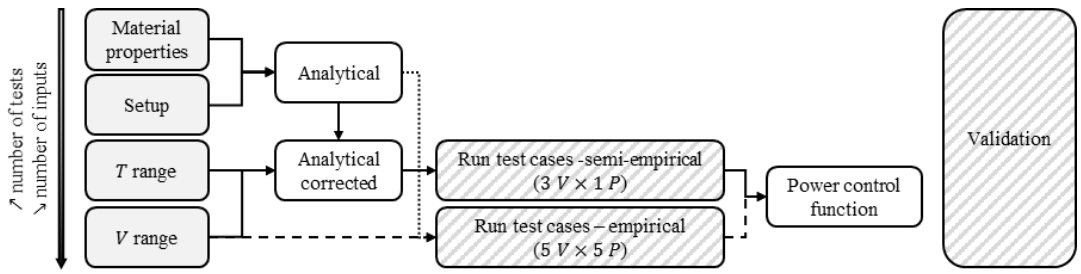

Figure 8. Power control function process flows for the empirical (plain arrows), semi-empirical (dashed arrows) and the combined analytical/ empirical procedures (dotted arrows).

The required inputs for the different processes are represented by plain boxes. The steps requiring computing are represented by white boxes and the experimental trials by hatched boxes. The semi-empirical power control function process (plain arrows), requires the largest number of inputs, but the lowest number of experiments. The empirical power control function process (dashed arrows), only requires the V operation range, but requires the largest number of experiments. The analytical process can be used to support the empirical process (dotted arrows) by determining the test cases (P,V).

6. Conclusions & future work

The presented study facilitates the implementation of the *humm3*™ heating system to layup composite parts by Automated Fibre Placement. It demonstrated that the heater power control function procedure developed by Di Francesco *et al.*'s can be applied to the bindered dry fibres/*humm3*™ combination (objective #1). It also showed that the *humm3*™ requires significantly more power than the diode laser to reach the same material temperature and that the power increment required to increase temperature by a certain amount is independent of layup speed. The substrate's more uniform through-thickness bulk temperature due to a larger headed area further away from the nip-point could explain these phenomena. Finally, it enables low cost deployment of the *humm3*™ technology for both manufacturing and R&D activities by defining a process flow that clearly indicates how the power control function can be determined depending on the input parameters' availability (material properties and setup) and the machine's time for conducting the experiments (objective #3). Future work in this field will include:

- Applying the method to the *humm3*™ when 2 or more of its parameters are changed at the time;
- Refining the presented methodology and combining it with numerical process modelling and accurate material characterisation to further reduce/eliminate the need for costly experiments;
- Standardising the experimental procedure, data acquisition and data processing to support industrial uptake.

Acknowledgments

This work was carried out at National Composites Centre (NCC) and is part of an Innovate UK funded project led by a consortium consisting of the NCC, Heraeus Noblelight Ltd and LMAT. The authors would like to thank Phil Druiff for his work on emissivity, which greatly contributed to the project.

Reference

[1] D. Lukaszewicz, C. Ward, K. Potter. The engineering aspects of automated prepreg layup: History, present and future. *Composites Part B: Engineering*, 43:997–1009, 2012.
[2] D. Williams and M. Brown. Xenon Flashlamp Heating for Automated Fibre Placement. *Third Int. Symp. on Automated Composites Manufacturing, Montreal, Canada,* April 20-21 2017.
[3] M. Di Francesco. *Laser-assisted Automated Fibre Placement process development,* 2017.
[4] M. Di Francesco, L. Veldenz, G. Dell'Anno and K. Potter. Heater power control for multi-material, variable speed Automated Fibre Placement. *Composites Part A: Applied Science and Manufacturing,* 101:408–421, 2017.
[5] HiTape™ brochure.
[6] Laserline. Diode laser manual; 2012.
[7] ASTM E1933-14: Standard Practice for Measuring and Compensating for Emissivity.
[8] A. Dasgupta and R. Agarwal. Orthotropic thermal conductivity of plain-weave fabric composites sing a homogenization technique. *J. of Composite Materials,* 26:2736—58, 1992.
[9] J. Wang, M. Gu, W. Ma, X. Zhang and Y. Song. Temperature dependence of the thermal conductivity of individual pitch-derived carbon fibers. *New Carb. Mat.,* 23:259—63, 2008.
[10] Y. Yang, F. Robitaille and S. Hind. Thermal conductivity of carbon fiber fabrics.*19th International Conference on Composite Materials, Montreal, Canada,* July 28-August 2 2013.
[11] I. Bass. Six sigma statistics with Excel and Minitab. McGrawn-Hill, 2007.